Gasser, D., Grenne, T., Corfu, F., Bøe, R., Røhr, T.S., and Slagstad, T., 2021, Concurrent MORB-type and ultrapotassic volcanism in an extensional basin along the Laurentian Iapetus margin: Tectonomagmatic response to Ordovician arc-continent collision and subduction polarity flip: GSA Bulletin, https://doi.org/10.1130/B36113.1.

Supplemental Material

Analytical methods. PDF file with description of the analytical methods.

Figure S1. Whole-rock geochemical plots for eight quartz dioritic clasts from the Skjøla olistostrome and comparison with the composition of the similarly aged Fagervika pluton in the underlying LVB ophiolite (Slagstad et al., 2014). Chondrite and primitive-mantle values from Sun and McDonough (1989). Slightly higher contents of incompatible elements and a negative Eu anomaly in the Fagervika pluton can be ascribed to its more evolved composition; volatile-free SiO_2 contents of the Fagervika pluton are ~77–80 wt%, vs. ~63–77 wt% in the Skjøla clasts.

Figure S2. (A) Concordia plot for zircon U–Pb TIMS data for sample C1 (TGR_441), a quartz dioritic clast from the Skjøla olistostrome (Figs. 2C, 3B). Data-point ellipses are 2σ; plot is made with Isoplot (Ludwig, 2003). (B) The zircons from this sample are euhedral prisms, relatively rich in U and strongly corroded during chemical abrasion. Three zircon fractions were analyzed, one with five grains, one with two grains and one with one grain (Table S2). The five-grain fraction is slightly discordant and appears to be affected by a slight amount of inheritance. The other two fractions give overlapping concordant results with a mean $^{206}Pb/^{238}U$ age of 478±1 Ma. This is within error of the geochemically similar Fagervika pluton dated at 481±3 Ma (Slagstad et al., 2014).

Figure S3. Whole-rock geochemistry plots of three porphyritic volcanic clasts of the Raudhatten conglomerate, compared to the shoshonitic Hølonda Porphyrites located farther northwest (Fig. 2B); Hølonda Porphyrite data from Grenne and Roberts (1998) and Slagstad et al. (2014). Chondrite and primitive-mantle values from Sun and McDonough (1989).

Figure S4. MORB-type rocks of the Ilfjellet Group. (A) Th/Yb vs. Mg#. Mg# for primary mantle melts after Niu and O'Hara (2008) and for average MORB after White and Klein (2014). (B) Nb/Yb vs. TiO_2/Yb diagram (Pearce, 2008). Symbols and average MORB and OIB compositions as in Fig. 6. (C) MORB-normalized (Sun and McDonough, 1989) Nb vs. Th diagram. Red outline shows typical compositions of back-arc basin basalts (BABB). The Ilfjellet Group MORBs plot outside of the typical BABB field or, partly, in the field of overlapping MORB-BABB compositions. Simplified after Saccani (2015).

Figure S5. Extended mantle-normalized trace element diagrams. Normalizing primitive-mantle values from Sun and McDonough (1989).

Figure S6. Microphotographs of zircon grains dated by U–Pb TIMS.

Table S1. Complete whole-rock geochemical data for analyzed samples of the Ilfjellet Group, along with quartz dioritic clasts from the Skjøla olistostrome and porphyritic volcanic clasts of the Raudhatten conglomerate.
Table S2. U–Pb TIMS zircon analyses.
Table S3. Nd and Sr isotope data.
Table S4. U–Pb LA–ICP–MS analyses of detrital zircons.

ANALYTICAL METHODS

Whole-rock geochemistry

Highly vesicular, sheared or otherwise obviously altered varieties were avoided during sampling. All samples were trimmed of weathered surfaces and veins prior to crushing and milling. Whole rock geochemical analyses were done at the Geological Survey of Norway (NGU). A PANalythical Axios 4kW XRF spectrometer with a Rh X-ray tube was used for major elements (measured on glass beads fused with Li2B4°7) and trace elements (measured on pressed powder pellets). Additional selected traces, including Rare Earth Elements (REE), were obtained by LA–ICP–MS on the same glass beads as were prepared for XRF. This was performed on a Thermo Fisher Scientific ELEMENT XR single collector high resolution ICP–MS coupled to a New Wave UP193FX Excimer 193 nm laser. All analyses used common international standards for calibration and duplicate analyses for quality control. Selected representative analyses, including major and trace elements referred to in the text, are shown in Table 1; a complete data set is provided in Supplemental Information, Table S1.

Sr and Nd isotope analysis

Dissolution and column chemistry

150–200 mg of sample was weighed into 15ml Savillex teflon beakers and leached in 5 mililiters of 6M HCl at 60 °C for 2 h. After discarding the leachate, the samples were washed and centrifuged twice in Type 1 mQ water, dried and reweighed. 1–2 ml of 2x quartz- distilled 16M HNO3 and 5–6 ml of 29M HF were added, and the sample beakers were left closed on a hotplate at 140 °C overnight. After evaporating to dryness, a further 1–2 ml of HNO3 was added, and the samples were left on the hotplate closed overnight. The samples were then converted to chloride form using 10 ml of Teflon-distilled HCl. The samples were then dissolved in c. 2 ml of calibrated 2.5M HCl in preparation for column chemistry, and centrifuged.

Separation of Sr and bulk REE

Samples from the primary column separation were dried down and taken up in c. 2 ml of 2.5M HCl and pipetted onto quartz-glass columns containing 4 ml of AG50x8 cation exchange resin. Matrix elements were washed off the column using 48 ml of calibrated 2.5M HCl and discarded. Sr was collected in 12 ml of 2.5M HCl and evaporated to dryness. A bulk rare-earth element fraction was collected in 15 ml of 6M HCl and evaporated to dryness.

Separation of Nd from the bulk REE fraction

Sm and Nd were separated using 2 ml of EICHROM LN–SPEC ion exchange resin packed into 10 ml Biorad Poly-Prep columns. The bulk REE fraction was dissolved in 200 microlitres of 0.2M HCl and loaded onto the columns. La, Ce and Pr were eluted using a total of 14 ml of 0.2M HCl. Nd was collected in 3 ml of 0.3M HCl.

Mass spectrometry

Nd analysis. Nd fractions were loaded onto one side of an outgassed double Re filament assembly using dilute HCl and analyzed in a Thermo Scientific Triton mass spectrometer in multi- dynamic mode. Data are normalized to $^{146}Nd/^{144}Nd = 0.7219$. Eleven analyses of the BCR–2 standard gave a value of 0.512628 ± 0.000016 (1σ). Results are quoted relative to a value of 0.512115 for the La Jolla standard.

Sr analysis. Sr fractions were loaded onto outgassed single Re filaments using a TaO activator solution and analyzed in a Thermo–Electron Triton mass spectrometer in multi-dynamic mode. Data are normalized to $^{86}Sr/^{88}Sr = 0.1194$. Seven analyses of the BCR–2 standard gave a value of 0.705003 ± 0.000018 (1σ). Sample data is normalized using a preferred value of 0.710250 for the NBS987 standard.

Geochronology

U–Pb TIMS

Zircons were separated using standard magnetic and heavy liquid techniques. Zircons were examined and selected under a binocular microscope and subsequently either chemically abraded (Mattinson, 2005) by annealing for 3 days at 900 °C, and then partial dissolution in HF (+HNO_3) at 190 °C for ca. 14 h, or air abraded (Krogh, 1982). The grains chosen for analysis were spiked with a mixed ^{202}Pb–^{205}Pb–^{235}U tracer that has recently been calibrated to the Earthtime (ET) 100 Ma solution (Ballo et al., 2019). After spiking, the zircons were dissolved in HF (+HNO_3) at ca. 195 °C for 5 days in Krogh-type bombs. The solutions of fractions larger than 1 μg were processed through ion exchange resin to purify U and Pb (Krogh, 1973). Details of the mass spectrometric techniques and parameters used are given in Augland et al. (2010) and Ballo et al. (2019). Ages were plotted and calculated using ISOPLOT (Ludwig, 2003), the decay constants of Jaffey et al. (1971) and $^{238}U/^{235}U$ according to Steiger and Jäger (1977).

U–Pb LA–ICP–MS

Zircon separation was conducted at the Geological Survey of Norway, where conventional magnetic and heavy liquid techniques were used to separate zircons. Individual zircon crystals were handpicked under a binocular microscope, mounted in epoxy and polished down to expose the grain centers. Backscatter (BSE) and cathodoluminescence (CL) images of the zircons were obtained prior to analysis using a Leo 1450 VP Scanning Electron Microscope (SEM) with a wolfram filament at the Geological Survey of Norway. The laser ablation inductively coupled plasma mass spectrometry (LA–ICP–MS) was performed using a New Wave UP193FX Excimer laser coupled to a Thermo Element XR single collector high resolution ICP–MS at the Geological Survey of Norway. A 15μm wide line scan at a speed of 2μm/sec was used at energies of 4.0 J/cm2 and a repetition rate of 10 Hz. Ca 0.4 l/min He gas was used as a carrier gas flushing through the sample chamber, mixed with ca 0.9 l/min Ar gas and transported to the ICP–MS. The measurement time was first 30 s of gas blank acquisition and thereafter up to 30 s data acquisition. Masses ^{202}Hg, $^{204}Hg + ^{204}Pb$, ^{206}Pb, ^{207}Pb, ^{208}Pb, ^{232}Th and ^{238}U were acquired in a time-resolved counting scanning mode. ^{235}U was recalculated from the natural abundance for $^{238}U/^{235}U$ (Steiger and Jäger, 1977). The measured isotope ratios were corrected for element- and mass-bias effects using the zircon standard GJ (607 ± 0.4 Ma; Jackson et al., 2004). The following zircon standards and reference zircons were used as control samples: 91500 (1065 ± 0.3 Ma; Wiedenbeck et al., 1995), Temora II (416.5 ± 0.22 Ma; Black et al., 2004), ØS-99–14 (1797 ± 3 Ma; Skår, 2002), Z6412 (1160 ± 1.6 Ma; unpublished, GSC Ottawa) and T33187 (2674 ± 8; unpublished in-house standard, NGU) were used for standardization. The data were not corrected for common Pb, but the signal from ^{204}Pb is used to exclude analyses containing common Pb. The data reduction was done with the GLITTER® software version 4.4.4 (Van Achterbergh et al., 2001). U–Pb ages of the zircons were calculated using the ISOPLOT software for Microsoft Excel version 3 (Ludwig, 2003), and Kernel density estimates and histograms of provenance ages were made with the detzrcr software package for R (Andersen et al., 2018).

Multiple methods have been proposed for calculating a MDA, the most commonly used being the youngest single grain (YSG), the youngest grain cluster composed of three or more grains that overlap at 2σ (YGC 2σ) and the youngest graphical peak (YPP; e.g., Dickinson and Gehrels, 2009; Coutts et al., 2019). There is no recommendation for discordance filtering included in the description of these methods (Dickinson and Gehrels, 2009), but we apply a 5% central discordance filter for our Paleozoic populations.

REFERENCES CITED

Andersen, T., Kristoffersen, M., and Elburg, M.A., 2018, Visualizing, interpreting and comparing detrital zircon age and Hf isotope data in basin analysis – a graphical approach: Basin Research, v. 30, p. 132–147, https://doi.org/10.1111/bre.12245.

Augland, L.E., Andresen, A., and Corfu, F., 2010, Age, structural setting, and exhumation of the Liverpool Land eclogite terrane, East Greenland Caledonides: Lithosphere, v. 2, p. 267–286, https://doi.org/10.1130/L75.1.

Ballo, E.G., Augland, L.E., Hammer, Ø., and Svensen, H., 2019, A new age model for the Ordovician (Sandbian) K-bentonites in Oslo, Norway: Palaeogeography, Palaeoclimatology, Palaeoecology, v. 520, p. 203–213, https://doi.org/10.1016/j.palaeo.2019.01.016.

Black, L.P., Kamo, S.L., Allen, C.M., Davis, D.W., Aleinikoff, J.N., Valley, J.W., and Foudoulis, C., 2004, Improved 206 Pb/238 U microprobe geochronology by the monitoring of a trace-element-related matrix effect; SHRIMP, ID–TIMS, ELA–ICP MS and oxygen isotope documentation for a series of zircon standards: Chemical Geology, v. 205, p. 115–140, https://doi.org/10.1016/j.chemgeo.2004.01.003.

Coutts, D.S., Matthews, A., and Hubbard, S.M., 2019, Assessment of widely used methods to derive depositional ages from detrital zircon populations: Geoscience Frontiers, v. 10, p. 1421–1435, https://doi.org/10.1016/j.gsf.2018.11.002.

Dickinson, W.R., and Gehrels, G.E., 2009, Use of U–Pb ages of detrital zircons to infer maximum depositional ages of strata: A test against a Colorado Plateau Mesozoic database: Earth and Planetary Science Letters, v. 288, p. 115–125, https://doi.org/10.1016/j.epsl.2009.09.013.

Jackson, S.E., Pearson, N.J., Griffin, W.L., and Belousova, E.A., 2004, The application of laser ablation-inductively coupled plasma-mass spectrometry to in situ U–Pb zircon geochronology: Chemical Geology, v. 211, p. 47–69, https://doi.org/10.1016/j.chemgeo.2004.06.017.

Jaffey, A.H., Flynn, K.F., Glendenin, L.E., Bentley, W.C., and Essling, A.M., 1971, Precision measurement of half-lives and specific activities of ^{235}U and ^{238}U: Physical Reviews, Section C: Nuclear Physics, v. 4, p. 1889–1906, 10.1103/PhysRevC.4.1889.

Krogh, T.E., 1973, A low contamination method for hydrothermal decomposition of zircon and extraction of U and Pb for isotopic age determinations: Geochimica et Cosmochimica Acta, v. 37, p. 485–494, https://doi.org/10.1016/0016-7037(73)90213-5.

Krogh, T.E., 1982, Improved accuracy of U-Pb zircon ages by the creation of more concordant systems using an air abrasion technique: Geochimica et Cosmochimica Acta, v. 46, p. 637–649, https://doi.org/10.1016/0016-7037(82)90165-X.

Ludwig, K.R., 2003, Isoplot 3.0. A geochronological toolkit for Microsoft Excel: Berkeley Geochronology Center Special Publication No. 4, 70 p.

Mattinson, J.M., 2005, Zircon U-Pb chemical abrasion ("CA-TIMS") method: Combined annealing and multi-step partial dissolution analysis for improved precision and accuracy of zircon ages: Chemical Geology, v. 220, p. 47–66, https://doi.org/10.1016/j.chemgeo.2005.03.011.

Pearce, J.A., 2008, Geochemical fingerprinting of oceanic basalts with applications to ophiolite classification and the search for Archean oceanic crust: Lithos, v. 100, p. 14–48, https://doi.org/10.1016/j.lithos.2007.06.016.

Skår, Ø., 2002, U–Pb geochronology and geochemistry of early Proterozoic rocks of the tectonic basement windows in central Nordland, Caledonides of north- central Norway: Precambrian Research, v. 116, p. 265–283, https://doi.org/10.1016/S0301-9268(02)00026-8.

Steiger, R.H., and Jäger, E., 1977, Subcommission on geochronology—convention on use of decay constants in geochronology and cosmochronology: Earth and Planetary Science Letters, v. 36, p. 359–362, https://doi.org/10.1016/0012-821X(77)90060-7.

Van Achterbergh, E., Ryan, C.G., Jackson, S.E., and Griffin, W.L., 2001, Data reduction software for LA–ICP–MS: Laser–Ablation–ICPMS in the earth sciences—principles and applications [short course series]: Mineralogical Association of Canada, v. 29, p. 239–243.

Wiedenbeck, M.A.P.C., Alle, P., Corfu, F., Griffin, W.L., Meier, M., Oberli, F., and Spiegel, W., 1995, Three natural zircon standards for U-Th-Pb, Lu-Hf, trace element and REE analyses: Geostandards Newsletter, v. 19, p. 1–23, https://doi.org/10.1111/j.1751-908X.1995.tb00147.x.

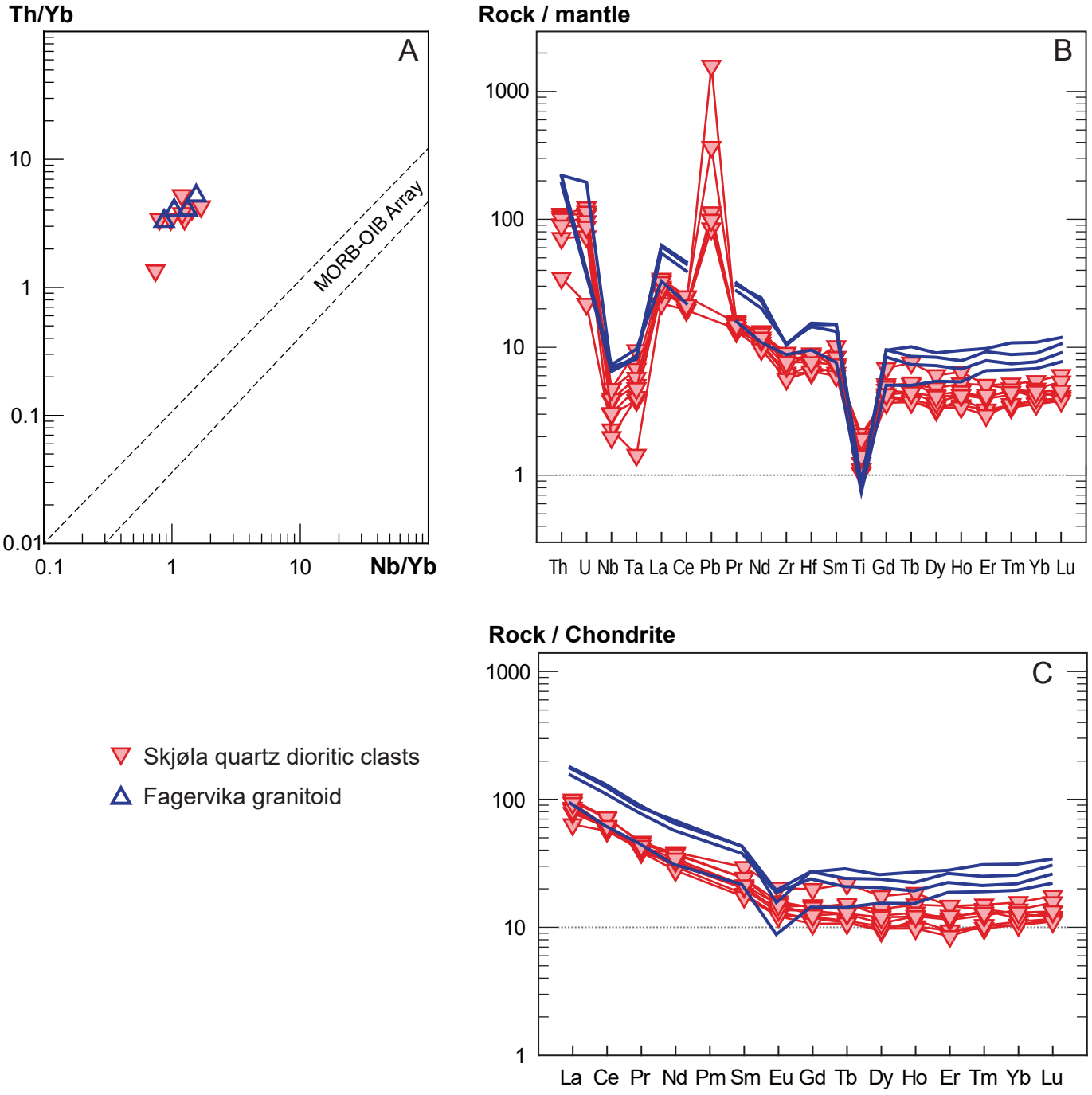

Figure S1. Whole rock geochemical data from eight quartz dioritic clasts from the Skjøla olistostrome, and comparison with the composition of the similarly-aged Fagervika pluton in the underlying LVB ophiolite (Slagstad et al., 2014). (A) Th/Yb vs. Nb/Yb plot. (B) Primitive mantle-normalized patterns. (C) Chondrite-normalized REE patterns. Chondrite and primitive mantle values from Sun and McDonough (1989). Slightly higher contents of incompatible elements and a negative Eu anomaly in the Fagervika pluton can be ascribed to its more evolved composition; volatile-free SiO2 contents of the Fagervika pluton are ~77–80%, vs. ~63–77% in the Skjøla clasts.

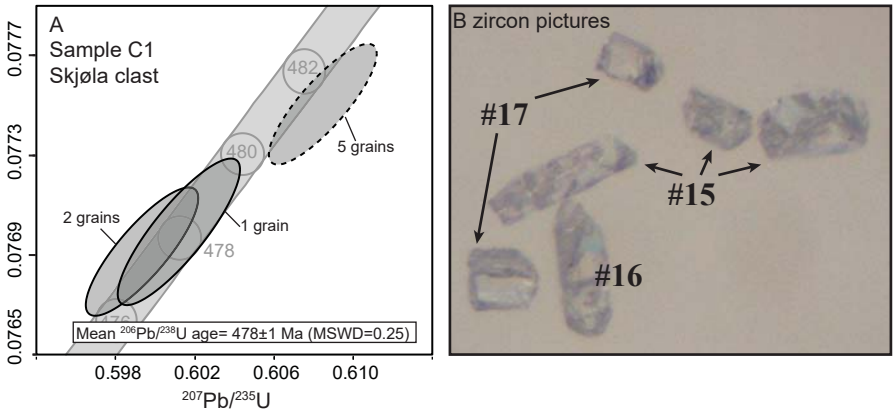

Figure S2. (A) Concordia plot for zircon U–Pb TIMS data for sample C1 (TGR_441), representing a granodioritic clast from the Skjøla conglomerate (Figs. 2c, 3b). Data-point ellipses are 2σ; plot is made with Isoplot (Ludwig 2003). (B) The zircons from this sample are euhedral prisms, relatively rich in U and strongly corroded during chemical abrasion. The three grains of #15 further fragmented into five grains during final cleaning. Three zircon fractions were analysed, one with five grains (#15), one with two grains (#17) and one with one grain (#16, Table S2). The five-grain fraction is slightly discordant and appears to be affected by a slight amount of inheritance. The other two fractions give overlapping concordant results with a mean 206Pb/238U age of 478±1 Ma. This is within error of the geochemically similar Fagervika pluton dated at 481±3 Ma (Slagstad et al., 2014).

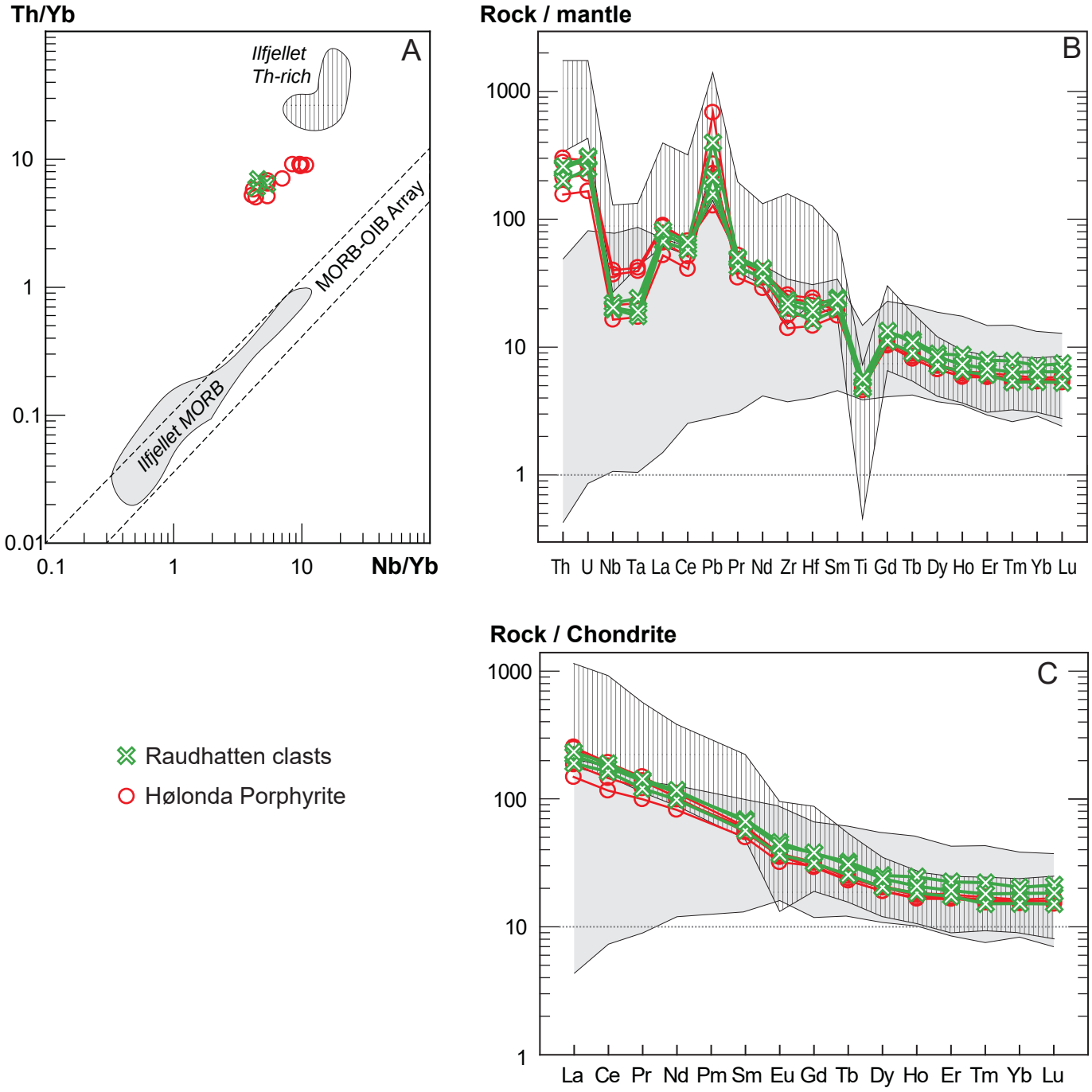

Figure S3. Whole rock geochemistry plots of three porphyritic volcanic clasts of the Raudhatten conglomerate, compared to the shoshonitic Hølonda Porphyrites located further northwest (Fig. 2b); Hølonda Porphyrite data from Grenne and Roberts (1998) and Slagstad et al. (2014). (A) Th/Yb vs. Nb/Yb plot. (B) Primitive mantle-normalized patterns. (C) Chondrite-normalized REE patterns. Chondrite and primitive mantle values from Sun and McDonough (1989). The clasts fir perfectly with the composition of the Hølonda Porphyrites, including negative Nb–Ta and positive Pb anomalies, and are distinctly different from the Ilfjellet Th-rich units as well as the Ilfjellet MORB-type lavas.

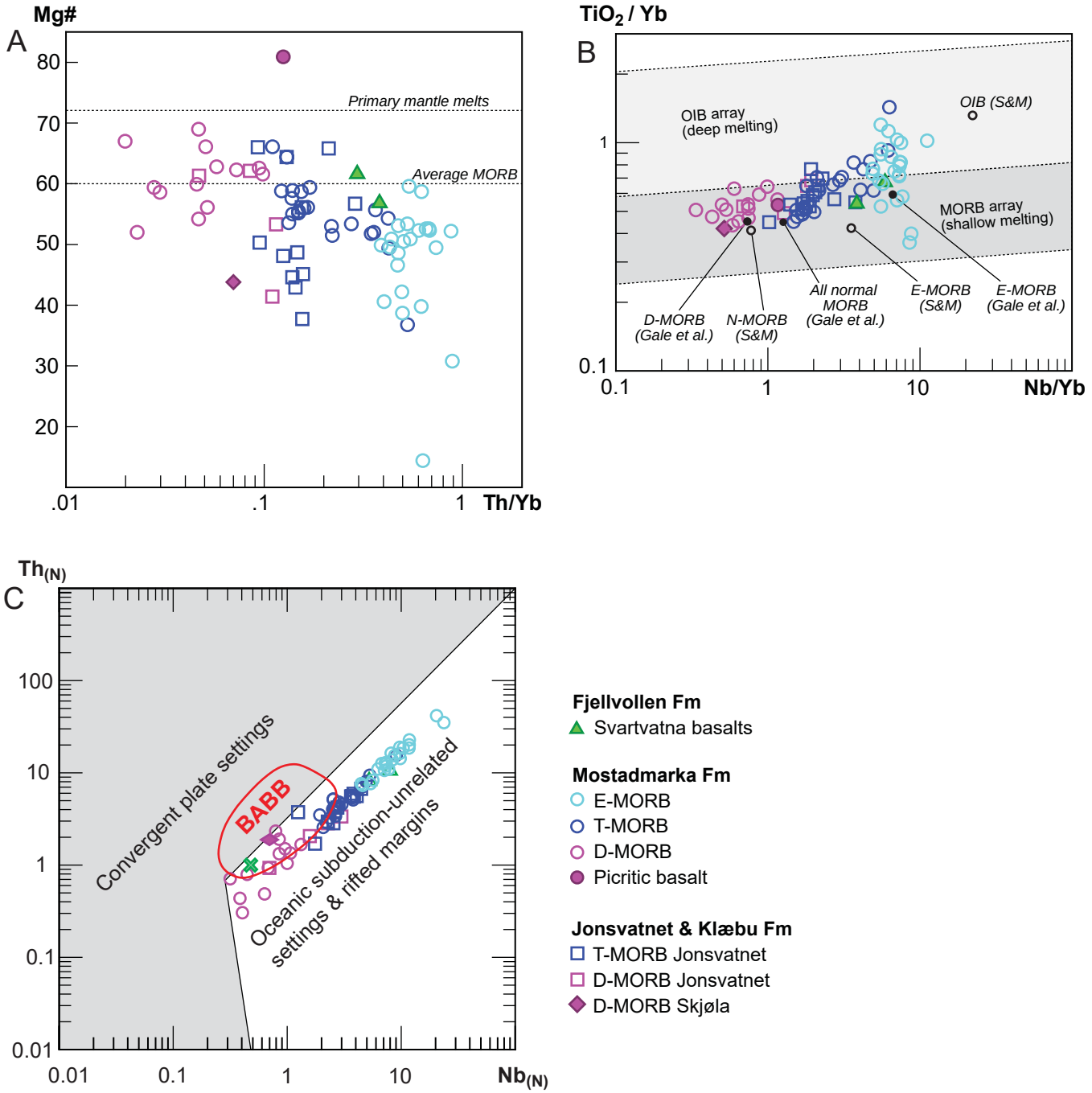

Figure S4. MORB-type rocks of the Ilfjellet Group.
(A) Th/Yb vs. Mg#. Mg# for primary mantle melts after Niu and O'Hara (2008) and for average MORB after White and Klein (2014).
(B) Nb/Yb vs. TiO2/Yb diagram (Pearce, 2008). Symbols and average MORB and OIB compositions as in Fig. 6.
(C) MORB-normalized (Sun and McDonough, 1989) Nb vs. Th diagram. Red outline shows typical compositions of back-arc basin basalts (BABB). The Ilfjellet Group MORBs plot outside of the typical BABB field or, partly, in the field of overlapping MORB-BABB compositions. Simplified after Saccani (2014).

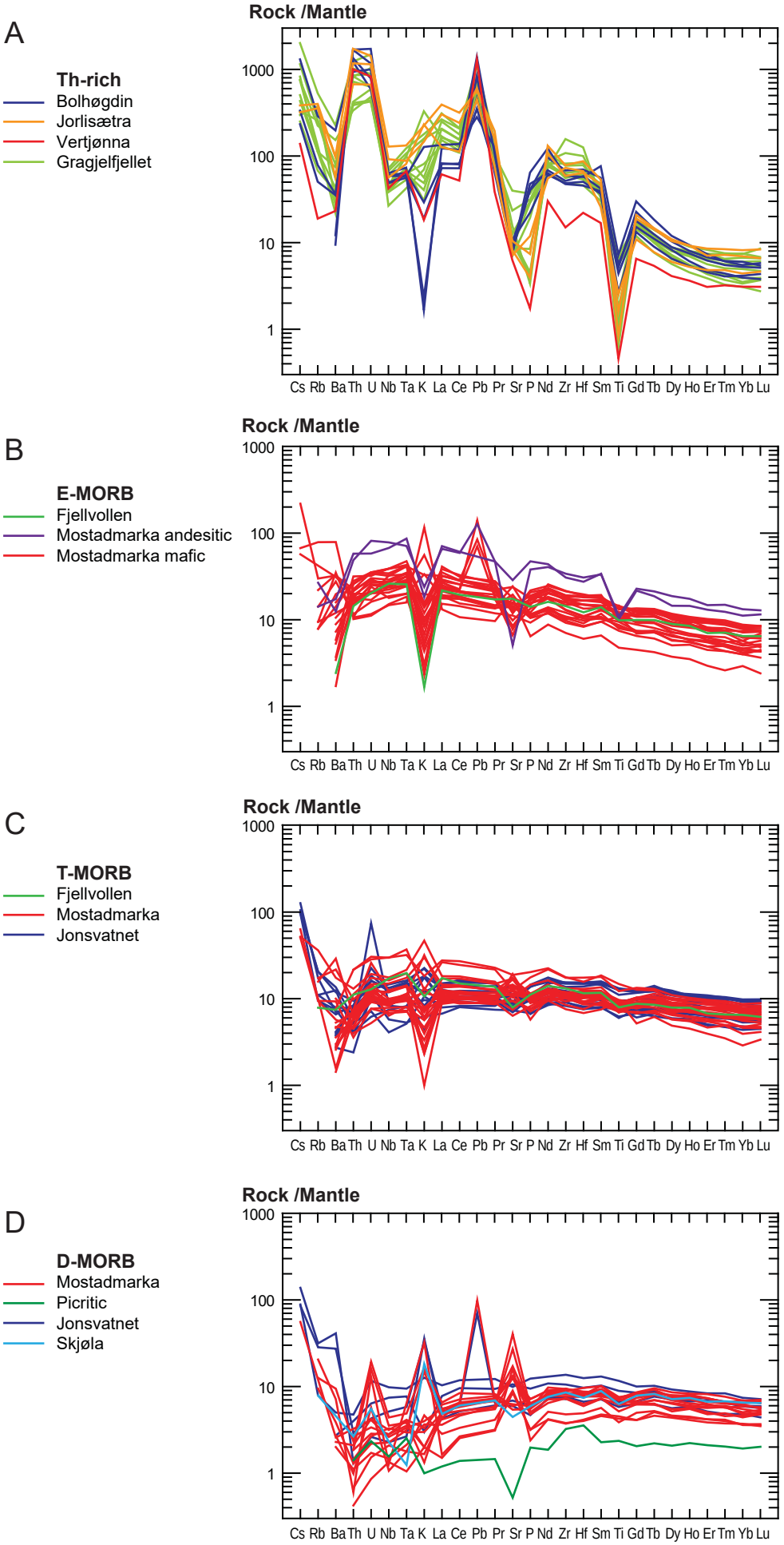

Figure S5. Extended mantle-normalized trace element diagrams. Normalizing values from Sun and McDonough (1989).

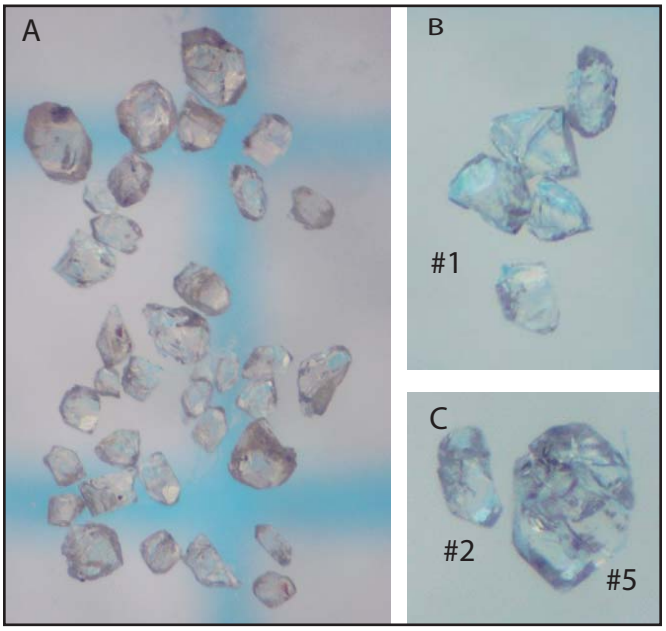

Sample V1 (TGR16_305)
Gragjelfjellet trachytic lava flow or dome
(A) Zircons before chemical abrasion.
(B) Clean grains selected for fraction #1.
(C) Grains #2 and #5, the latter underwent a slight Pb loss, probably related to the internal imperfections.

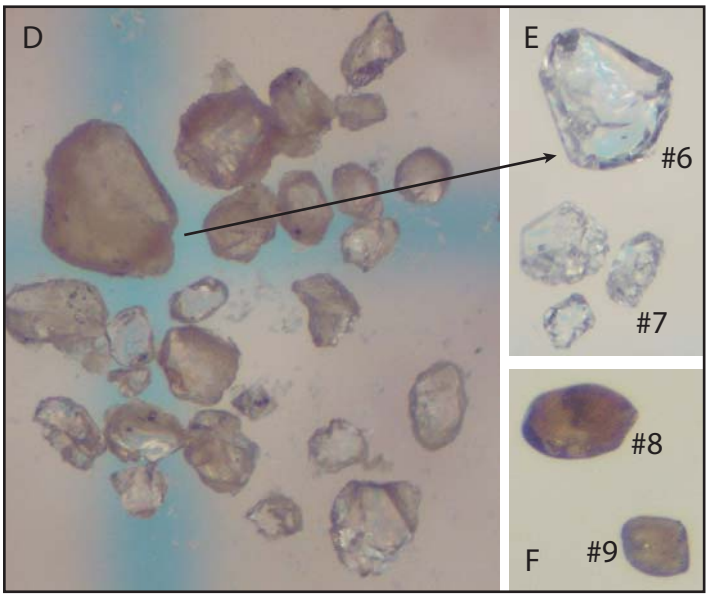

Sample V2 (TGR14_223)
Jorlisætra trachytic tuff
(D) clear to brownish zircons before chemical abrasion, mostly fragments, but locally euhedral faces.
(E) Zircons selected for analyses #6 and #7. Grain 6 yields the oldest and most reliable age of 473±1 Ma.
(F) The two brown grains #8 and #9, rich in U.

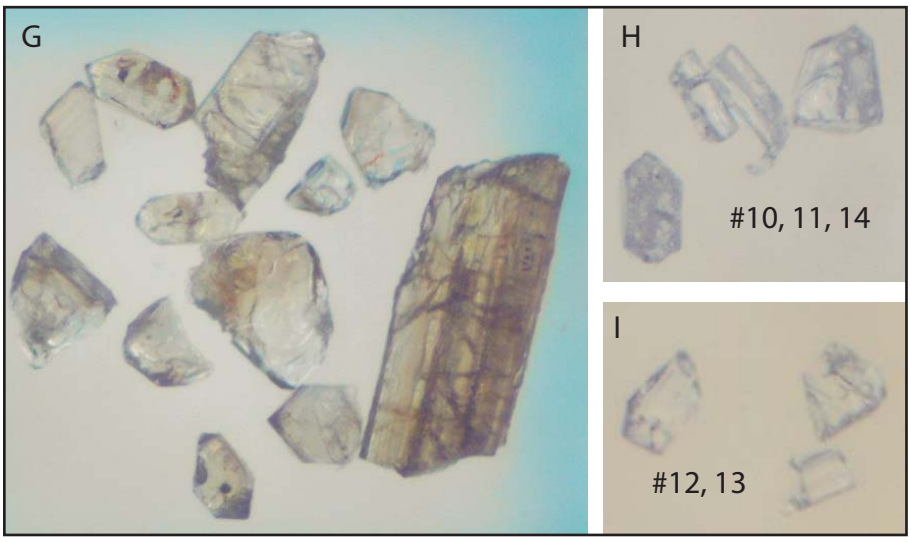

Sample V3 (TGR15_408)
Bolhøgdin trachytic lava
(G) Zircons before chemical abrasion - euhedral crystals and fragments. (H) clean grains selected for analyses #10, #11 and #14. (I) Grains used for #12 and #13. Due to the high U content and metamictization the grains were strongly attacked during chemical abrasion and few fragments were left.

Figure S6. Microphotographs of zircon grains dated by U-Pb TIMS.